A Membrane Bending Model of Outer Hair Cell Electromotility

Robert M. Raphael,* Aleksander S. Popel,* and William E. Brownell†

*Department of Biomedical Engineering, Center for Hearing Sciences and Center for Computational Medicine and Biology, The Johns Hopkins University School of Medicine, Baltimore, Maryland 21205 and †Bobby R. Alford Department of Otorhinolaryngology and Communicative Sciences, Baylor College of Medicine, Houston, Texas 77030 USA

ABSTRACT We propose a new mechanism for outer hair cell electromotility based on electrically induced localized changes in the curvature of the plasma membrane (flexoelectricity). Electromechanical coupling in the cell's lateral wall is modeled in terms of linear constitutive equations for a flexoelectric membrane and then extended to nonlinear coupling based on the Langevin function. The Langevin function, which describes the fraction of dipoles aligned with an applied electric field, is shown to be capable of predicting the electromotility voltage displacement function. We calculate the electrical and mechanical contributions to the force balance and show that the model is consistent with experimentally measured values for electromechanical properties. The model rationalizes several experimental observations associated with outer hair cell electromotility and provides for constant surface area of the plasma membrane. The model accounts for the isometric force generated by the cell and explains the observation that the disruption of spectrin by diamide reduces force generation in the cell. We discuss the relation of this mechanism to other proposed models of outer hair cell electromotility. Our analysis suggests that rotation of membrane dipoles and the accompanying mechanical deformation may be the molecular mechanism of electromotility.

INTRODUCTION

Inside the mammalian cochlea are outer hair cells, which possess the ability to convert electrical energy to mechanical energy and generate force at acoustic frequencies greater than 50 kHz (Frank et al., 1999). These outer hair cells play an indispensable role in hearing, enabling sharp frequency discrimination at low sound intensities by supplying energy to the cochlear partition. The electromechanical coupling in the outer hair cell, referred to as electromotility, was first observed by Brownell and coworkers (Brownell et al., 1985) and was subsequently further investigated and quantified (Ashmore, 1987; Santos-Sacchi, 1991, 1992, 1993). Its paramount importance in auditory physiology has been the subject of many recent reviews (Nobili et al., 1998; Dallos, 1997; Ashmore, 1994; Brownell and Popel, 1998; Lim and Kalinec, 1998). Loss or damage to outer hair cells can cause high-frequency hearing loss, and at least one form of inherited deafness is due to a defective membrane channel in the outer hair cells (Kubisch et al., 1999).

Outer hair cell electromotility is unique among biological motile mechanisms in the speed at which it operates. For most motile mechanisms in biology, we now have at least some knowledge of the molecules involved. However, the molecular mechanism of electromotility remains unknown. Among the different biophysical models that have been proposed for electromotility, the two-state molecular motor model adequately accounts for most experimental observations. In its most general form, this model postulates that a motor molecule exists that changes its conformation between two states when the cell's membrane potential is changed (Dallos et al., 1993). The cell is cylindrically shaped, and the model postulates that the motor molecule gives rise to different strains in the longitudinal and circumferential direction of the cell without specifying any requirements on the cell surface area. In other versions of this model, the conformational change is explicitly specified to be an area change (Iwasa, 1994; Santos-Sacchi, 1993). A change in shape as a result of the application of an electric field is a phenomenon known in solid crystals as piezoelectricity, and formal piezoelectric models of outer hair cell motility have been proposed (Mountain and Hubbard, 1994; Tolomeo and Steele, 1995; Spector, 1999; Spector et al., 1999a,b).

The above models do not explicitly take into account the complex trilamellar structure of the outer hair cell's lateral wall. Electron microscopy reveals that the cochlear outer hair cell has a unique multilayered membrane structure (See Fig. 1). The outermost layer, the plasma membrane, appears corrugated or folded in electron micrographs (Smith, 1968; Furness and Hackney, 1990; Ulfendahl and Slepecky, 1988, Dieler et al., 1991; Holley et al., 1992). Extending from the plasma membrane into the cytosol are structures of unknown composition referred to as "pillars" (Forge, 1991). The folds in the membrane appear to anchor at the pillars. The pillars form a connection between the plasma membrane and the cytoskeleton because they are attached to circumferential actin filaments. The actin filaments are crosslinked by thinner filaments (spectrin molecules), which are oriented preferentially in the longitudinal direction of the cell. Beneath the cytoskeleton is another membraneous layer referred to as the subsurface cisterna (SSC). It is not known if this layer is connected to the cytoskeleton. In contrast to the plasma membrane, the SSC appears

Received for publication 30 August 1999 and in final form 7 March 2000.

Address reprint requests to Robert M. Raphael, Johns Hopkins University School of Medicine, Department of Biomedical Engineering, 720 Rutland Ave, Baltimore, MD 21205. Tel.: 410-955-1787; Fax: 410-614-8796; E-mail: rraphael@bme.jhu.edu.

0006-3495/00/06/2844/19 $2.00

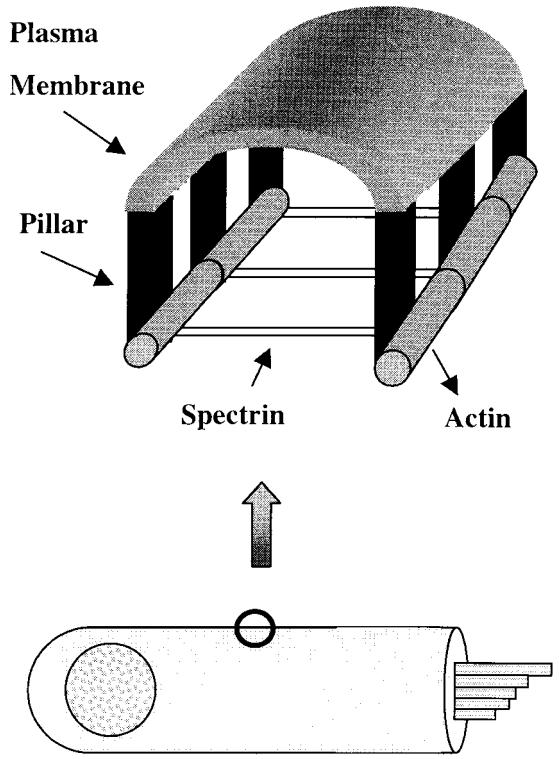

FIGURE 1 A schematic of the outer hair cell. These cells are cylindrically shaped with lengths ranging from 20 to 90 μm along the cochlea and with a radius of 4–5 μm. The hair bundle, composed of stereocilia, is located at the apex of the cell. The lateral wall is the source of electromotility and it appears smooth under a light microscope. When examined with electron microscopy, the lateral wall appears corrugated. The folds in the membrane appear to terminate at pillar proteins that extend to the cytoskeleton. The cytoskeleton is composed of actin filaments crosslinked by spectrin molecules.

smooth in electron micrographs (Dieler et al., 1991; Saito, 1983). A complete model of outer hair cell electromotility should consider the lateral wall's unique ultrastructural composition.

In this work, we propose a model of electromotility that is based on the structure of the lateral wall and the following considerations:

1. membranes are thin structures in which bending deformations play a pivotal role in the response to external forces;
2. membranes are liquid crystals and exhibit flexoelectricity;
3. the plasma membrane and the cytoskeleton are tightly associated.

The phospholipid and protein molecules that comprise biological membranes give the membrane the material property of having a large resistance to area changes (Bloom et al., 1991). From the perspective of thin films, membranes are in a condensed phase characterized by high surface pressure and tight packing of molecules. However, due to their thinness, membranes have a small resistance to bending, which can barely be measured experimentally. The bending resistance of the membrane is close to the Boltzmann thermal energy (kT), and, as a result, bending of pure giant vesicles (Servuss et al., 1976; Schneider et al., 1984) and red cell flickering (Strey et al., 1995) can be driven by thermal fluctuations in the environment and observed microscopically.

The second important consideration for our model of electromotility is that biological membranes are liquid crystals (de Gennes, 1974; Collings, 1990). Liquid crystals are distinguished from solid crystals in that the molecules of solids display positional and orientational order, whereas the molecules of liquid crystals display only orientational order. In biological membranes, the constituent phospholipid and protein molecules not connected to the cytoskeleton, packed at high density or confined in domains, are free to diffuse laterally so there is no positional order, but the molecules are constrained to remain preferentially aligned with their long axis perpendicular to the membrane, which gives the structure an orientational order.

Liquid crystals exhibit a unique coupling between applied electric fields and mechanical deformation. This effect, termed "flexoelectricity," is caused by the curvature-induced electrical polarization of the material. Though first presented as a peculiar kind of piezoelectricity to explain "unusual effects" observed in liquid crystals (Meyer, 1969), flexoelectricity is fundamentally different from the piezoelectric effect observed in solid crystals. Theoretically, flexoelectricity is based on the realization that out-of-plane bending of a liquid crystal will alter the electric field inside the material. Petrov (1975) hypothesized that phospholipid membranes, being liquid crystals, should exhibit flexoelectricity. In particular, biological membranes are composed of protein and lipid molecules that have large dipole moments parallel to their axes, a requirement for flexoelectricity. Experimentally, it has been confirmed in black lipid membranes that membrane polarization changes when the membrane curvature is changed (the flexoelectric response) (Petrov, 1999; Todorov et al., 1994a). Sun (1997) also demonstrated that flexoelectricity can be induced by the pressure from sound waves and is sensitive to membrane composition. However, flexoelectricity is bi-directional, and so, in addition to this mechanoelectrical coupling, flexoelectric materials should also exhibit an electromechanical coupling. Electromechanical transduction in lipid membranes has been observed experimentally (Todorov et al., 1994b). This direct bending of a membrane as a result of the application of an electric field is sometimes referred to as the "converse flexoelectric effect." This converse flexoelectric effect has been invoked to explain voltage-dependent movements in cells observed with atomic force microscopy (Mosbacher et al., 1998).

The plasma membrane of most eukaryotic cells is connected to an underlying cytoskeleton. The cytoskeleton is

responsible for structural support of the cell and contains elements that resist deformation. In the red blood cell and the outer hair cell, the cytoskeleton comprises a network of spectrin and actin molecules. In both these cells, experiments have demonstrated a tight association between the plasma membrane and the cytoskeleton (Hwang and Waugh, 1997; Oghalai et al., 1998). The bending of one layer of a multilayered composite membrane can transmit deformation and force to another component. In a discussion of the mechanics of multilayered membranes, Evans and Skalak (1980) proposed that "if the layers are strongly associated, then couples of force resultants between layers can be produced which create a moment resultant." Evans and Skalak also noted that the moment resultant could be the dominant response to external forces. Because the outer hair cell lateral wall is a strongly associated multilayered system, we will present an analysis of how the deformation in the plasma membrane results in a deformation of the cortical lattice. We will show that an active bending element can function as a cellular motor by transmitting forces to an elastic cytoskeletal element.

These considerations will lead us to a formulation of a "membrane-bending" model of outer hair cell electromotility. This model will show that electrically induced local bending of the membrane (flexoelectricity) can phenomenologically describe experimental observations of outer hair cell electromotility. A flexoelectric mechanism would also enable force generation at high frequencies. In addition, the model will account for the isometric force generated in the cell and explain experimental results, such as the weakening of force production in diamide-treated cells. The model explicitly provides for constant (or nearly constant) cell surface area and gives a pivotal role to localized membrane curvature changes, the importance of which is increasingly being realized in cell biology.

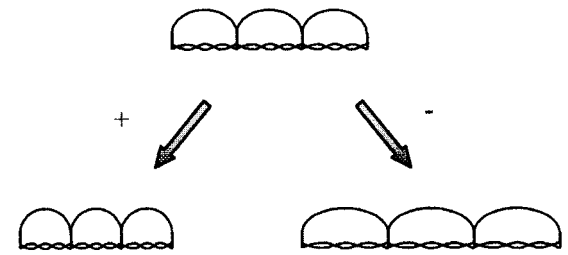

FIGURE 2 Micromechanical model for membrane deformation. Curvature changes in the elemental motile unit cause extension of the spectrin molecules attached to the pillars. Three units are shown in the figure. A depolarization (+) leads to a decrease in the radius of curvature and a shortening of the cell and hyperpolarization (−) leads to an increase in the radius of curvature and cell lengthening.

THE MODEL

The micromechanical picture

We define the elemental motile unit of electromotility as the plasma membrane and associated cytoskeleton between adjacent pillar proteins (See Fig. 2). In particular, the curvature of the plasma membrane between the pillars coupled with the length of spectrin comprises an elemental structural unit in the cell. The curvature of the plasma membrane between the pillars is able to change, and these curvature changes will be induced by alterations in the transmembrane potential. An increase in the curvature causes the membrane to fold up and will shorten the cell, whereas a decrease in curvature causes the membrane to flatten and will elongate the cell, as illustrated in Fig. 2. Possible molecular mechanisms responsible for these curvature changes are discussed later. The result of decreasing the curvature of the plasma membrane is to increase the spacing between the actin filaments and elongate the extensible spectrin molecules. Figure 3 illustrates the geometry for analyzing this curvature deformation. In Appendix A, we derive the geometric relationship between the curvature change and the longitudinal elongation.

These structural units of motility are spaced along the entire length of the lateral wall. The motile units are connected in series, as required by evidence from microchamber experiments that the magnitude of the voltage-induced cell displacement increases from the point at which the cell in inserted in the microchamber in a cumulative manner (Dallos et al., 1991). This electromechanical system is mechanically characterized as a bending element in parallel with a linear elastic element. The bending modulus of the membrane is denoted k_c and the spring constant of the elastic element is denoted k_s. For simplicity, we only analyze membrane deformation in the longitudinal direction, which experimental evidence shows is the primary mode of action of the motor (Dallos et al., 1991). However, a small

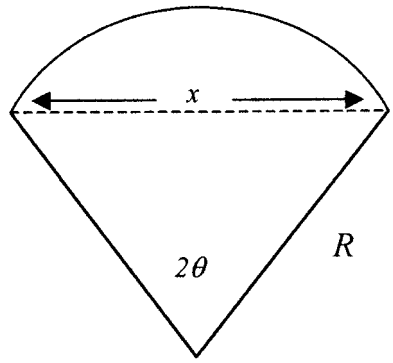

FIGURE 3 Geometry for analyzing membrane deformation. The membrane contour follows a smooth arc with a radius of curvature R. Curvature changes map to an equivalent longitudinal deformation x, which is related to the polar angle. See Appendix A for the relationship between these parameters.

change in the radius of the cell accompanies the length change.

Plasma membrane mechanical properties

The membrane is treated as a two-dimensional elastic material. In the analysis that follows, we restrict ourselves to the postulated elemental unit, which is modeled as a thin ring-shaped shell wrapped around the circumference of the cell. It is assumed that the shell undergoes pure bending. The classical theory of thin shells defines the moment produced by bending as (Timoshenko and Woinowsky-Kreiger, 1959)

$$M_p = \int_{-h/2}^{h/2} \sigma z \, dz, \tag{1}$$

where σ is the stress, h is the thickness of the shell, and z is the direction normal to the shell (see Fig. 4). The subscript p stands for passive. Note that M_p is a moment resultant: it is the sum of the torques about the neutral surface of the membrane. It has the units of force because it is the moment divided by length (force $\times$ length/length). The implicit length specified in this definition of the moment is the arc length of the half shell (see Fig. 3).

In the analysis of Evans and Skalak (1980), the product of the bending stiffness of the membrane and the total curvature gives the force produced by bending the membrane,

$$M_p = k_c(c_l + c_\varphi - c_o), \tag{2}$$

where k_c is the bending rigidity, c_l is the curvature of the membrane in the longitudinal direction, c_φ is the curvature of the membrane in the circumferential direction and c_o is the spontaneous curvature of the membrane. The spontaneous curvature describes any intrinsic tendency of the membrane to curve in the absence of applied external forces and is related to the molecular composition of the membrane.

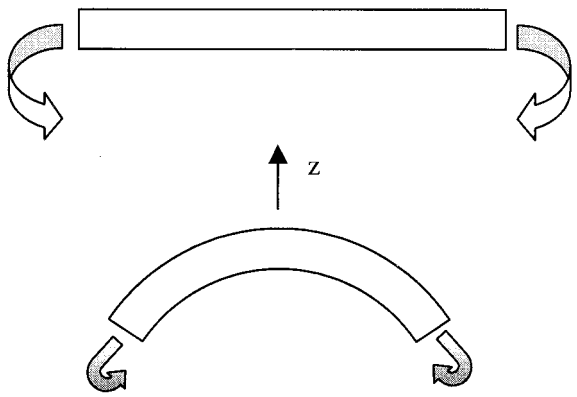

FIGURE 4 Illustration of parameters used to define the bending moment. An initially undeformed sheet of membrane of thickness h is subjected to a torque about its edges. This force causes out-of-plane bending of the material. The z direction is normal to the membrane. See Eq. 1.

The bending rigidity is related to the area expansivity modulus, K, of the membrane by the relationship (Waugh et al., 1992),

$$k_c = \frac{Kh^2}{12}, \tag{3}$$

where h is the membrane thickness. In the energetic formalism, the bending energy density is the Helfrich elastic energy for curvature deformation in a liquid crystal (Helfrich, 1973),

$$\tilde{E}_b = \tfrac{1}{2} k_c(\bar{c} - c_o)^2, \tag{4}$$

where $\bar{c} = c_l + c_\varphi$ is the sum of the membrane curvatures. In bilayer membranes, there will be an additional energy arising from differential expansion and compression in the membrane that occurs during bending (Evans, 1974). At present, we neglect this energetic contribution in our model of outer hair cell electromotility. The magnitude of this nonlocal bending energy is of the same order as the local bending energy (Raphael and Waugh, 1996).

Spectrin mechanical properties

The result of changing the membrane curvature will be to change the interpillar distance and elongate or shorten the spectrin molecules. The spectrin molecules will essentially form an elastic element that is in parallel with the bending element (see Fig. 2). The spectrin molecules are represented as a system of springs and the energy stored in the spectrin network is written as

$$\tilde{E}_{sp} = \tfrac{1}{2} n_{sp} k_s (x - x_o)^2, \tag{5}$$

where k_s is the spring constant, x_o is the resting (unstressed) length of the molecule and n_{sp} is the number of springs (spectrin molecules) per unit area.

Passive mechanical energy and equilibrium

The internal energy of the membrane–spring system is equated to the mechanical work done by deformation. In our micromechanical model, this work is due to bending of the plasma membrane and extension of the spectrin molecule s. The mechanical work per unit area due to deformation is written as

$$\tilde{U}_m = \tfrac{1}{2} k_c(c_l - c_o)^2 + \tfrac{1}{2} k_s n_{sp}(x - x_o)^2. \tag{6}$$

Note that this expression only considers deformation in the longitudinal direction in the membrane. In a complete model of electromotility, the curvature change in the circumferential direction will be linked to the deformation of

the actin molecules. Because these changes are small, we neglect them as a first approximation. Because the bending and the extension are related geometrically, the bending and extensional terms can be combined into an effective mechanical term, as described in Appendix A. Effectively, the spring displacement x is linearized about the curvature c_l resulting in a relationship,

$$x = a + b(c_l - c_o), \tag{7}$$

where a and b are constant terms.

The equilibrium of the membrane–spring system can be calculated by setting the partial derivative of the internal energy equal to zero. The resulting relationship between the curvature and the spring length in terms of the ratio of the elastic constants for bending and extension is

$$c_e = c_o - \frac{k_s n_{sp} b(a - x_o)}{k_c + k_s n_{sp} b^2}. \tag{8}$$

This relationship specifies the equilibrium configuration of the membrane–spring system. Given the elastic constants, the resting spring length, and the spontaneous curvature, the equilibrium curvature and spring length are then determined. These parameters will thus specify the resting (equilibrium) state of the elemental unit. We note that it is possible that the bending of the membrane may be compressing the spectrin molecules, or that the spectrin may be inducing membrane curvature. In terms of the equilibrium curvature, the internal energy can be rewritten as (See Appendix A)

$$\begin{aligned}\tilde{U}_m &= \tfrac{1}{2}(k_c + k_s n_{sp} b^2)(c_l - c_e)^2 + G \\ &= \tfrac{1}{2} k_{eff}(c_l - c_e)^2 + G,\end{aligned} \tag{9}$$

where k_{eff} is the effective bending stiffness and G is a constant term defined in Appendix A. For convenience, the internal energy can be redefined, omitting the constant term, as

$$\tilde{U}_m = \tfrac{1}{2} k_{eff}(c_l - c_e)^2. \tag{10}$$

Alternatively, the curvature can be expressed in terms of the spring length x in Eq. 7, and the energy can be expressed in terms of an effective spring stiffness.

Force generation during displacement from equilibrium

Because the motile unit is composed of an elastic element in parallel with a bending element, the total passive force per unit length in the longitudinal direction that a single elemental unit exerts will be the sum of the forces from the bending element and the elastic element:

$$F_t = F_b + F_{sp}. \tag{11}$$

The effective longitudinal displacement of the bending element is equal to the displacement of the spectrin molecules. We locate an active flexoelectric element in the plasma membrane. Hence, passive and active elements in the plasma membrane are in parallel with the elastic element representing the spectrin molecules. To evaluate the force generated in our micromechanical model, we now consider the properties of an active, voltage-sensitive bending element.

Electrically-induced curvature changes

Biological membranes are composed of protein and lipid molecules that possess dipole moments that establish an electric field within the membrane. Hence, the membrane shell will contain dipoles, as illustrated in Fig. 5. These dipoles give the shell an internal electric field and consequently a polarization. The application of an external electric field changes the curvature of the membrane (the converse flexoelectric response). The relationship between the applied electric field, the orientation of the dipoles in the membrane and the resulting curvature is illustrated in Fig. 5.

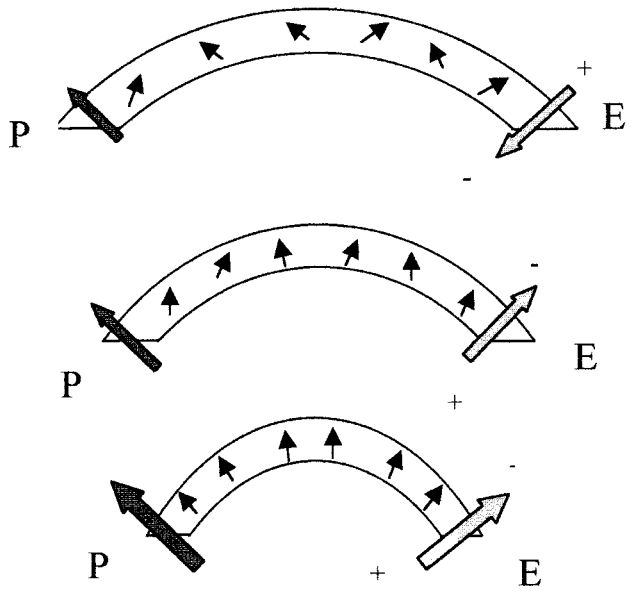

FIGURE 5 Orientation of dipoles in the membrane. This figure displays the effect of altering the external electric field on the molecular dipoles and, consequently, the curvature and polarization of the membrane. The magnitude and direction of the polarization vector (**P**) and electric field vector (**E**) are illustrated as arrows at the left and the right of a curved element of membrane. The top panel illustrates a hyperpolarized membrane in which the molecular dipoles have rotated to minimize the polarization opposed to the applied field. This corresponds to the largest radius of curvature. The middle panel represents a slightly depolarized membrane, at which more of the dipoles are aligned with the field and the polarization is increased. The bottom panel represents a maximally depolarized membrane, in which all the dipoles are aligned with the applied field. This corresponds to the largest curvature and the shortest length of the motile unit.

Note that we have assumed a simple picture of flexoelectricity as originating from the rotation of dipoles in analogy with liquid crystals. In real biological membranes the situation can be more complicated because dipoles, quadrupoles, and surface charges contribute to the polarization (Petrov and Sokolov, 1986; Petrov, 1999). Petrov (1975) first proposed the mathematical relationship between the membrane curvature and the membrane polarization,

$$P_s = f(c_1 + c_\varphi) = f\bar{c}, \tag{12}$$

where P_s represents the magnitude of the surface polarization vector per unit area, f is the flexoelectric coefficient with units of Coulombs (C), c_1 represents the membrane curvature in the longitudinal direction, and c_φ is the curvature in the circumferential direction. The sign of the flexoelectric coefficient f is positive when P_s points outward from the center of curvature of the membrane and negative when it points inward (Petrov, 1999).

Below, we derive the fundamental equations of flexoelectricity in an analogous manner to that done for piezoelectric materials. We then apply these equations to our model of outer hair cell electromotility. In the treatment of piezoelectricity, a thermodynamic potential called the electric enthalpy per unit area is defined, which is written as (Cady, 1946; Meyer, 1969; Lines and Glass, 1977),

$$\tilde{H} = \tilde{U} - ED_s, \tag{13}$$

where $\tilde{U}$ is the total internal energy per unit area, E is the electric field, and D_s is the electric displacement. The internal energy contains contributions from both the mechanical energy described earlier and the electrical energy,

$$\tilde{U}_{el} = \tfrac{1}{2}\,\varepsilon_o E^2, \tag{14}$$

where ε_o is the permittivity of free space. The electric displacement per unit length is written as

$$D_s = h\varepsilon_o E + P_s = h\varepsilon_o E + f\bar{c}, \tag{15}$$

where h is the thickness of the membrane. Combining the above equations, we define the electric enthalpy per unit area to be

$$\tilde{H} = \tfrac{1}{2}\,k_{eff}(c_1 - c_e)^2 - \tfrac{1}{2}\,h\varepsilon_o E^2 - f\bar{c}E. \tag{16}$$

The derivative of the electric enthalpy with respect to curvature defines the moment resultant in the membrane,

$$M = \frac{\partial \tilde{H}}{\partial c_1} = k_{eff}(c_1 - c_e) - fE. \tag{17}$$

Note the moment resultant has units of force (N). The total moment resultant is thus the sum of passive bending resistance and active flexoelectric properties. The derivative of the electric enthalpy, with respect to the electric field, defines the charge displacement for the two dimensional membrane,

$$D_s = -\frac{\partial \tilde{H}}{\partial E} = f\bar{c} + \varepsilon_o hE. \tag{18}$$

The charge displacement has units of C/m. Eq. 18 predicts that alterations in membrane curvature will produce charge displacement in the membrane.

Eqs. 17 and 18 represent the fundamental electromechanical coupling equations that will be used in our micromechanical model of outer hair cell electromotility. They are analogous to those derived for linear piezoelectric materials (Cady, 1946). They are also analogous to the equations presented by Tolomeo and Steele (1995) in their piezoelectric model of outer hair cell motility. However, in our treatment, the bending stiffness replaces the area elastic modulus, the curvature replaces the areal strains and the flexoelectric coefficient replaces the piezoelectric coefficient. In addition, our electrical energy (D_sE) is defined per unit area and not per unit volume. This corresponds to defining the electric displacement per unit length and not per unit area, as is the case in Tolomeo and Steele (1995). The treatments are equivalent when Eq. 18 is divided by the membrane thickness (h). Note that, if we express the curvature c_1 in terms of the spectrin length using Eq. 7, the model appears phenomenologically piezoelectric with the equations equivalent to the previous piezoelectric models. However, the biophysical meaning of the terms in the present model is different.

Nonlinear flexoelectric model

The above analysis assumed a linear relationship between membrane polarization and membrane deformation, as originally proposed by Petrov (1975). However, in our physical model illustrated in Fig. 5, the flexoelectric response saturates when all the membrane dipoles are aligned in the direction of the applied field. Hence, we extend Petrov's original formulation to include nonlinear effects. For a collection of dipoles, the fraction of the dipoles oriented in the direction of the applied field is given by the Langevin function (Cady, 1946). The Langevin function is defined as

$$\mathcal{L}(\xi) = \mathrm{Coth}(\xi - \xi_o) - \frac{1}{(\xi - \xi_o)}. \tag{19}$$

A derivation of the Langevin function is presented in Appendix B. This function is illustrated graphically in Fig. 6. The argument of the function is $\xi = p_o E_p/kT$, where p_o is the permanent dipole moment and E_p is the polarizing or local field. The term ξ_o is introduced to account for the spontaneous polarization. The membrane will exhibit a polarization in the absence of an applied field because the molecular dipoles are sterically constrained to remain oriented about one direction in the membrane. The existence of

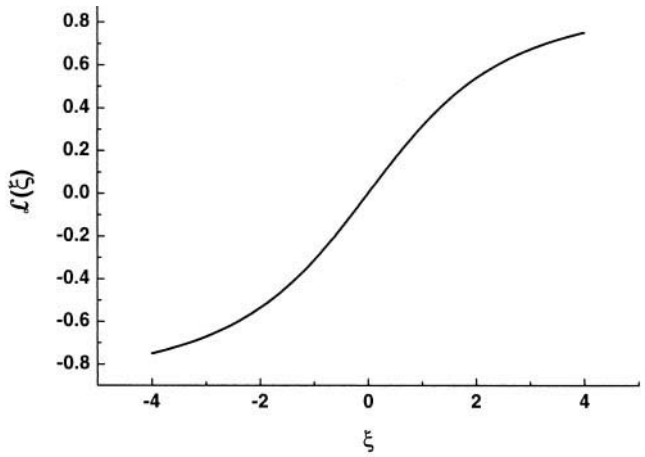

FIGURE 6 The Langevin function. This function describes the distribution of dipoles aligned with a field as a function of the polarizing field. At low fields, the function is linear, but becomes nonlinear as the field intensity increases. The function saturates when all of the dipoles are aligned in the direction of the field.

this spontaneous electric field will account for the offset in the electromotility function from zero. Note that the Langevin function enters a nonlinear region when the argument becomes larger than 1.5 and then approaches saturation slowly. For molecules with small dipole moments, the nonlinear region is never reached at low fields and the linear relations presented earlier are valid. However, if molecules have a large dipole moment, or local fields become very large, the membrane polarization will no longer be a linear function of the electric field.

When the membrane polarization is a nonlinear function of the electric field, the polarization can be expressed as a power series:

$$P_s(E) = \chi_1 E + \chi_2 E^2 + \cdots = f(E)\bar{c}, \tag{20}$$

where χ_1 and χ_2 are constants. A nonlinear relationship between the polarization and the electric field will translate into a nonlinear dependence of the flexoelectric coefficient on membrane potential. It has been mentioned in the flexoelectric literature that the flexoelectric coefficient can be voltage dependent (Hristova et al., 1991), yet a formal relationship has not been presented.

The thermodynamic potential in the nonlinear dielectric will take the form,

$$\begin{aligned}\tilde{H} &= \tilde{U}_m - \tfrac{1}{2} h\varepsilon_o E^2 - PE \\ &= \tilde{U}_m - \tfrac{1}{2} h\varepsilon_o E^2 - f(E)E\bar{c}.\end{aligned} \tag{21}$$

Note that the energy will now include a nonquadratic term that arises from the product of the polarization and the electric field. The existence of a nonquadratic term in the thermodynamic potential was postulated by Spector (1999) in his electroelastic model of outer hair cell motility. The nonlinear charge enthalpy per unit area is written as

$$\tilde{H} = \tfrac{1}{2} k_{eff}(c_l - c_e)^2 - \tfrac{1}{2} h\varepsilon_o E^2 - f(E)E\bar{c}. \tag{22}$$

The product $f(E)E$ represents the force that orients the dipoles when a field is applied. This flexoelectric force acts on the membrane to change its curvature. This force is proportional to the fraction of dipoles oriented with the applied field at a given value of the field, so the product $f(E)E$ is written as a constant multiplied by the Langevin function,

$$f(E)E = f_o \mathcal{L}(\xi). \tag{23}$$

Using this relationship, the moment resultant will be written in the nonlinear case as

$$M = \frac{\partial \tilde{H}}{\partial c_l} = k_{eff}(c_l - c_e) - f_o \mathcal{L}(\xi). \tag{24}$$

The relationship for the charge displacement can be derived by noting that the product of the polarization and the electric field is given by a constant times the Langevin function,

$$PE = P_{max} \mathcal{L}(\xi)E, \tag{25}$$

where $P_{max} = Np_o$, with N being the number of dipoles per unit area. From this, it follows that the charge displacement is

$$D_s = -\frac{\partial \tilde{H}}{\partial E} = 2P_{max}\mathcal{L}(\xi) + h\varepsilon_o E. \tag{26}$$

We note that the charge displacement will contain both linear and nonlinear terms. Eq. 24 will be used to describe the nonlinear features of outer hair cell motility, and Eq. 26 can be used to describe the nonlinear features of outer hair cell charge movement.

MODEL PARAMETERS AND FEASIBILITY

At the nanoscale level, we estimate that the plasma membrane of the outer hair cell follows an arc with a radius of curvature of about 30 nm between pillar proteins attached to adjacent circumferential (actin) filaments. The interactin (or interpillar) spacing is based on electron microscopic images of Forge (1991). The spacing between the circumferential filaments varies considerably and depends on the fixation buffer and method (Holley et al., 1992). Forge (1991) reported this interactin distance to be 36 nm, whereas Holley et al. (1992) reported that it can vary from 20 to 80 nm. The spectrin molecules crosslink the actin filaments at various angles, yet the average spacing between spectrin molecules is on the order of 10–30 nm and they are not always coincident with the pillars (Holley et al., 1992); the lengths of spectrin molecules range between 30 and 80 nm.

We investigate the feasibility of the membrane-bending model by determining whether the forces generated are sufficient to cause the experimentally measured deformations of the outer hair cell. We first discuss experimentally determined values of the parameters in the model and then determine whether these values make our micromechanical model feasible.

Values of electro-mechanical parameters

Flexoelectric coefficient

The value of the flexoelectric coefficient depends on the detailed molecular composition of the membrane. For zwitterionic lipids with no net charge, the magnitude of the coefficient is $\sim 10^{-20}$ C (Petrov and Usherwood, 1994). For a membrane with nonzero surface charge and fully ionized lipid head groups, the value of flexoelectric coefficient is much higher, $\sim 10^{-18}$ C (Todorov et al., 1994a). We will consider the bounds of the magnitude of the flexoelectric coefficient to be 10^{-20}–10^{-18} C. There are no physical constraints on the sign of the flexoelectric coefficient, though experiments indicate that it depends on the surface charge of the membrane (Petrov and Sokolov, 1986; Derzhanski et al., 1990). For the outer hair cell deformation, which requires a decrease in the curvature with membrane hyperpolarization, the flexoelectric coefficient must be positive.

Bending stiffness

The bending stiffness of the outer hair cell plasma membrane has not been directly experimentally measured. However, the bending stiffness of synthetic phospholipid membranes determined by various experimental techniques is on the order of $\sim 1.2 \times 10^{-19}$ J (Meleard et al., 1998; Raphael and Waugh, 1996). When cholesterol is incorporated into the membrane, the bending stiffness can be as large as 5×10^{-19} J (Song and Waugh, 1993). The presence of membrane proteins can either decrease or increase the bending stiffness slightly. For the red blood cell, the bending modulus has been measured to be 2.0×10^{-19} J (Hwang and Waugh, 1997). We adopt this value for the outer hair cell as a lower limit. We note that mechanical models of the entire lateral wall predict an effective bending stiffness three orders of magnitude higher (Spector et al., 1998). It is likely that this large resistance to bending for the entire wall is due to the stiff circumferential actin filaments or the subsurface cisterna. However, it is possible that the plasma membrane of the outer hair cell has a higher bending stiffness than that of a red blood cell, perhaps as large as 10^{-18} J. Hence, we take the range for the bending stiffness to be on the order of 2×10^{-19}–10^{-18} J. We note that a larger bending stiffness for the plasma membrane makes the model more feasible, provided enough force is generated by the flexoelectric mechanism. This issue will be discussed below.

Spectrin elasticity

The elasticity of the spectrin molecule in the outer hair cell has been estimated from the work of Tolomeo et al. (1996). They report the Young's modulus for spectrin to be 3×10^6 N/m^2. Assuming the spectrin molecule is 2.5 nm thick, this translates into an equivalent spring constant of $\sim 6 \times 10^{-3}$ N/m. However, Hansen et al. (1996) report the spectrin spring constant in the red blood cell to be on the order of $\sim 10^{-5}$ N/m, based on an elastic network model of the red cell membrane. In a more recent model by Boey et al. (1998), the effective spring constant of a spectrin network is reported to be $\sim 30\ kT/s_o^2$, where s_o is the force-free spring length. Assuming that the resting length of spectrin in the outer hair cell is ~ 40 nm, the effective spring constant will be 7.5×10^{-5} N/m. Hence, the reported spring constants of spectrin fall within the range $\sim 6 \times 10^{-5}$–10^{-3} N/m.

From the value of the bending stiffness and the spectrin elasticity, we can calculate the effective bending resistance k_{eff}. The parameter b defined in Appendix A is calculated assuming the equilibrium curvature to be 30 nm. The number of spectrin molecules per unit area is taken to be $n_{\text{sp}} = 2.5 \times 10^{15}$ m^{-2}. For $k_c = 2.0 \times 10^{-19}$ J and $k_s = 1.0 \times 10^{-3}$ N/m, k_{eff} is calculated to be 3×10^{-19} J. The values of the electromechanical parameters discussed above (f, k_c, and k_s) are summarized in Table 1.

Experimental voltage-to-length parameters

The feasibility of the model is evaluated for an outer hair cell 80 μm long. For such a cell, there will be approximately 2000 motile units (membrane folds as shown in Fig. 2)

TABLE 1 Values of electromechanical parameters

Parameter	Preparation	Value	References
f	Black lipid membranes	10^{-18}–10^{-20} C	Petrov and Usherwood, 1994
k_c	Giant vesicles	1.2×10^{-19} J	Raphael and Waugh, 1996 Meleard et al., 1998
	Red blood cells	2.0×10^{-19} J	Hwang and Waugh, 1997
k_s	Red blood cells	10^{-5} N/m	Hansen et al., 1996
		8×10^{-5} N/m	Boey et al., 1998
	Outer Hair Cells	6×10^{-3} N/m	Tolomeo et al., 1996

along the length. Here we have chosen the spacing between the actin filaments (the interpillar distance) to be 40 nm. A 10-mV hyperpolarization of the membrane potential would increase the cell length by a maximum 0.2 μm in accord with the maximum voltage-to-length function of 20 nM/mV (Santos-Sacchi, 1992). From this, we estimate the increase in the distance between the pillars to be 0.1 nm and calculate the increase in the radius of curvature geometrically via Eq. A2 in Appendix A. The result is that, for a 0.1-nm extension of a spectrin molecule, the radius of curvature will change from 30 to 30.4 nm. The angle θ defined in Fig. 3 will increase from 41.2 to 41.8 degrees.

Feasibility estimates

We now evaluate whether enough force is generated by the flexoelectric effect to bend the membrane and extend the spectrin molecule in this typical case.

Flexoelectricity. The linear constitutive relationship (Eq. 17) for the resting and 10-mV hyperpolarized membrane is written as

$$\begin{aligned} M_1 &= k_{\text{eff}}(c_1 - c_e) - fE_1\,, \\ M_2 &= k_{\text{eff}}(c_2 - c_e) - fE_2\,, \end{aligned} \tag{27}$$

where the subscripts 1 and 2 designate values of the quantities at their respective membrane potentials. In an unloaded cell, M does not change (there is no generation of force by the active mechanism), and the relation between the change in the electric field and the change in the curvature will be

$$\Delta E = E_2 - E_1 = \frac{k_{\text{eff}}}{f}(c_2 - c_1) = \frac{k_{\text{eff}}}{f}\left(\frac{1}{R_2} - \frac{1}{R_1}\right), \tag{28}$$

where R_2 and R_1 designate two states of the radius of curvature in the longitudinal direction, c_l. The change in curvature in the circumferential (φ direction), which reflects a change in the cell's radius, is extremely small and can be neglected.

We note that the electric field is related to the membrane potential V by the relationship $E = V/h$, when the potential is defined as the difference between the inside of the cell and the outside and h is the membrane thickness. This convention defines an inwardly directed field as negative, in agreement with the convention for the flexoelectric coefficient. Using the previous estimates of the change in the radius of curvature for a 10 mV hyperpolarization in the membrane potential, and taking the membrane thickness to be 5 nm and assuming it does not change, we calculate that the magnitude of k_{eff}/f should be $\sim$5 J/C. Because the value of the flexoelectric coefficient ranges from 10^{-20} to 10^{-18} C, we conclude that the effective bending resistance should be in the range $5 \times (10^{-20}$–$10^{-18})$ J, i.e., overlapping with the range of k_{eff} we identified above.

Membrane bending. The next question that arises is whether the force produced by membrane bending is sufficient to deform the spectrin spring. When the membrane curvature changes from an initial curvature c_1 to a new curvature c_2, the spectrin spring extends from an initial length x_1 to a new length x_2. The change in the bending energy of the membrane is then written as

$$\Delta\tilde{E}_b = \tfrac{1}{2}\,k_c(c_2^2 - c_1^2). \tag{29}$$

Likewise, from Eq. 5, the energy to change the conformation of spectrin molecules per unit area is

$$\Delta\tilde{E}_{sp} = \tfrac{1}{2}\,n_{sp}k_s(x_2^2 - x_1^2). \tag{30}$$

For the energy produced by bending of the membrane to be sufficient to extend the spectrin spring, the right-hand side of Eq. 29 must be greater than or equal to the right hand side of Eq. 30. For the parameters given, the range of the variation in the bending energy will be between 3×10^{-6} and 3×10^{-5} J/m^2 from Eq. 29. The range for the variation in the energy per unit area generated by spectrin will be 1.5×10^{-5}–10^{-7} N/m from Eq. 30. Hence, there is a range of parameters for which the force generated by bending is sufficient to deform the spectrin springs. Because the force generated by bending on a nanoscale is sufficient to deform the cytoskeleton, we will now move to predicting the microscopic cell deformations observed as a function of changes in the electric field.

MODEL PREDICTIONS

Length changes with voltage changes in the linear model

From the linear constitutive equation for the flexoelectric membrane, we can predict the length change in the outer hair cell as a function of the change in the transmembrane potential. For an unloaded motile unit that generates no force, Eq. 28 is rearranged to give

$$c_2 - c_1 = \frac{f\Delta V}{k_{\text{eff}}h}, \tag{31}$$

where $\Delta V = V_2 - V_1$. For depolarization, ΔV is positive, whereas for hyperpolarization, ΔV is negative. Note that ΔV represents the difference in membrane potential between two states, not the absolute value of the membrane potential.

When we substitute the geometric relationship between the change in membrane curvature and the longitudinal displacement derived in Appendix 1 (Eq. A4), we obtain

$$x_2 - x_1 = \frac{bf\Delta V}{k_{\text{eff}}h}, \tag{32}$$

where b is the conversion factor derived in Appendix A. The total length change in the cell, ΔL_{cell}, will be the above

equation multiplied by the number of folds, designated N_f. A prediction of ΔL_{cell} versus the change in transmembrane potential is plotted in Fig. 7. As shown, the model predicts maximal cell deformations of the order of a few microns over membrane potential changes consistent with voltage clamp measurements (Santos-Sacchi, 1991). The model also predicts that the slope of the voltage-to-length curve is dependent on the ratio of the effective bending stiffness to the flexoelectric coefficient. We illustrate this in Fig. 7 by showing the predictions for different values of k_{eff}/f, which effectively alters the gain of the electromotility function. Note that these predictions are symmetric with respect to the origin of both the length and voltage axes. The electromotility data, in addition to being nonlinear, is also skew symmetric about both axes. We deal with these issues in the nonlinear model discussed below.

Nonlinear outer hair cell length changes with voltage

The nonlinear flexoelectric model allows us to predict for the length change in the cell as a function of the polarizing field. For an unloaded cell that generates no force, Eq. 24 is written as

$$c_l - c_e = \frac{f_o \mathcal{L}(\xi)}{k_{eff}}. \tag{33}$$

The longitudinal displacement of the motile unit is related to the curvature change from the initial state by the geometric relationship derived in Appendix A (Eq. A4). The initial curvature is expressed in terms of the equilibrium curvature via Eq. A7. Combining these equations with Eq. 33, we obtain the relationship,

$$\Delta x = x - a = \frac{b}{k_{eff}}(f_o \mathcal{L}(\xi) - b k_s n_{sp}(a - x_o)). \tag{34}$$

This equation follows because a is the initial length of the motile unit at the initial curvature state. The prediction for the length change in the cell can be written as

$$\Delta L_{cell} = \Delta L_m \mathcal{L}(\xi) + \Delta L_{V0}, \tag{35}$$

where

$$\Delta L_m = \frac{N_f b f_o}{k_{eff}} \qquad \Delta L_{V0} = \frac{N_f b^2 k_s n_{sp}(x_o - a)}{k_{eff}}.$$

The parameter ΔL_{V0} is a bias term that accounts for the skew symmetry with respect to the length axis of the electromotility function. Its magnitude depends on the passive mechanical properties of the membrane, and its sign depends on the displacement of the spectrin spring from its force-free length at the initial curvature. If the spring is extended, then $x_0 < a$ and the electromotility curve is shifted downward. The saturating value of the length change when the Langevin saturates in the positive direction is equal to $\Delta L_m + \Delta L_{V0}$. Let us assume that our initial state is the force-free state of spectrin ($a = x_0$). The prediction for the electromotility curve is then given by Eq. 35 with $\Delta L_{V0} = 0$. The curve will follow the Langevin function, which is a function of the dipole moment and the polarizing field. A prediction of ΔL_{cell} versus the change in polarizing field is plotted in Fig. 8 for different values of the dipole moment p_o. This figure illustrates that, when the dipole moment is reduced, a transition from nonlinear to linear behavior is predicted in the experimental region of voltage clamp measurements. The predicted electromotility curves are centered at zero because we have, for now, assumed no spontaneous polarization. Thus, from Eq. 35, the parameter $f_o = k_{eff}\Delta L_m / N_f b$.

The spontaneous polarization ($E_{p,o}$) is accounted for by expressing the argument of the Langevin function in terms of the membrane potential as

$$\xi = \frac{p_0}{kT}(E_p - E_{p,o}) = \frac{p_0}{kT(1-\lambda)}\frac{1}{h}(V - V_0) = \gamma(V - V_0), \tag{36}$$

where $1 - \lambda$ is the conversion factor between the polarizing field and the applied field (See Appendix B).

The predictions of the membrane-bending model can now be compared to experimental observations to determine values of the parameters. In Fig. 9, we illustrate the result of a nonlinear least squares regression fit to the experimental data of Santos-Sacchi (1992). The data were fit to the equation

$$\Delta L_{cell} = \Delta L_m \mathcal{L}((\gamma(V - V_0)) + \Delta L_{V0}, \tag{37}$$

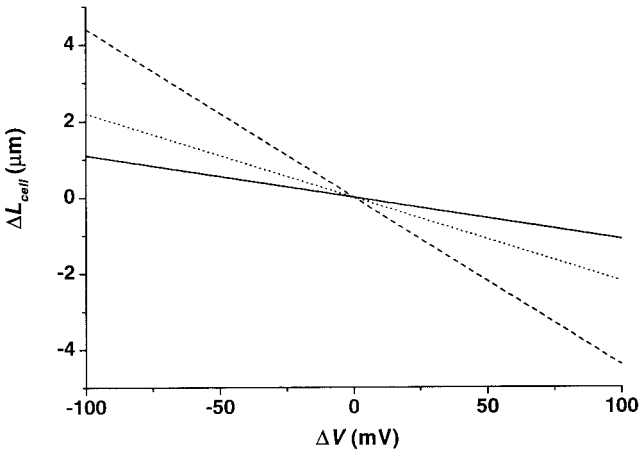

FIGURE 7 Length changes in the outer hair cell. The linear flexoelectric model predicts the length change as a function of transmembrane potential changes as shown here. The magnitude of the response depends on the ratio of the bending rigidity to the flexoelectric coefficient. We illustrate this for three different ratios: ——, $k_{eff} = 4 \times 10^{-19}$ J, $f = 1 \times 10^{-19}$ C; ····, $k_{eff} = 4 \times 10^{-19}$ J, $f = 2 \times 10^{-19}$ C; – – –, $k_{eff} = 4 \times 10^{-19}$ J, $f = 4 \times 10^{-19}$ C. Cell length increases with hyperpolarization and decreases with depolarization.

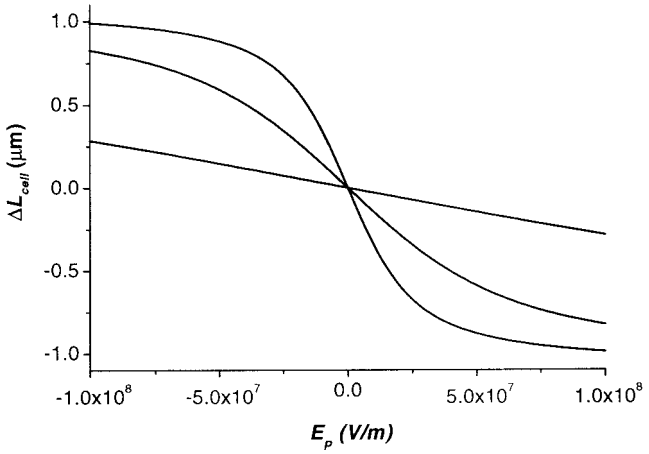

FIGURE 8 Nonlinear length changes in the outer hair cell as a function of molecular dipole moment. The nonlinear flexoelectric model predicts the slope of the length change as a function of polarizing field will depend on the value of the dipole moment. These curves were generated from Eq. 35 with the parameters $N_f = 2000$, $k_{eff} = 4 \times 10^{-19}$ J, $f_o = 1 \times 10^{-12}$ C/m, $\Delta L_{V0} = 0$. The value of the molecular moment was $p_o = 125$ D (*top*), $p_o = 50$ D (*middle*) and $p_o = 10$ D (*bottom*). The polarizing field 1×10^8 V/m corresponds to a membrane potential of 180 mV for $p_o = 125$ D, 372 mV for $p_o = 50$ D, and 474 mV for $p_o = 10$ D. (See Appendix B). Cell length increases as the polarizing field is increased and decreases as the polarizing field is decreased. Note that the direction of the polarizing field is opposite from the direction of the transmembrane potential, i.e., a positive polarizing field corresponds to a negative transmembrane potential.

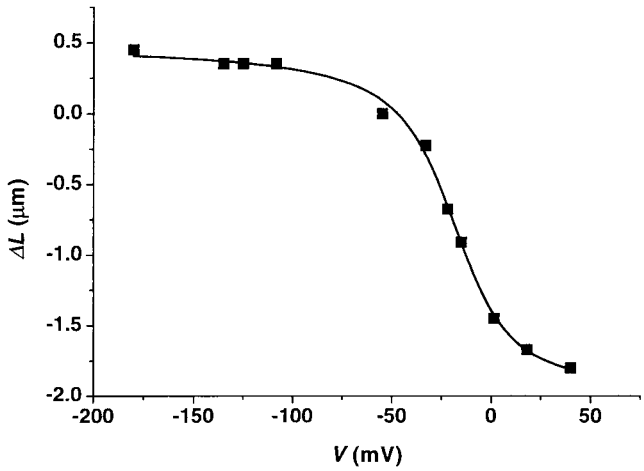

FIGURE 9 Nonlinear regression fit to experimental data. The solid points are the experimental data on electromotility reported by Santos-Sacchi (1992). The solid line is the nonlinear least squares regression fit to the experimental prediction. The nonlinear least squares regression was carried out according to the Levenberg-Marquardt algorithm using the software package Origin (Microcal, Inc.). The parameters are described in the text.

where ΔL_m, γ, V_0, and ΔL_{V0} were the free parameters of the fit. The nonlinear least squares regression yielded the results $\Delta L_m = -1.27$ μm, $\gamma = 0.09$ mV^{-1}, $V_0 = -29$ mV, and $\Delta L_{V0} = -0.78$ μm ($\chi^2 = 0.00274$). We now see that ΔL_{V0} accounts for the experimental observation that, at $V = V_0$, ΔL_{cell} is not equal to zero.

Isometric Force

The isometric force is the force generated when no deformation of the membrane occurs. The magnitude of the isometric force can be estimated from the linear flexoelectric model applying the condition $c_1 = c_e$ in Eq. 17. (Note that it is also possible to apply the same condition to Eq. 24 to calculate the isometric force in the nonlinear case). In this case, the active force is the flexoelectric coefficient multiplied by the electric field, fE. The active force per unit length of the membrane equals fE divided by the arc length of the motile unit ($s = 2R\theta$). This expression takes the form,

$$F_a = \frac{fE}{s} = \frac{fV}{sh}. \tag{38}$$

The coefficient of the active force is the derivative of the active force with respect to the membrane potential,

$$\frac{dF_a}{dV} = \frac{f}{sh}. \tag{39}$$

Assuming f to be 10^{-18} C, the coefficient of the active force evaluates to 4.5×10^{-3} N/Vm, a value similar to that reported by Spector et al. (1999a,b) and Spector (1999) for the longitudinal component of the force in the orthotropic electroelastic model. This coefficient can be converted to a coefficient in terms of force per voltage change by multiplying by the total length of a motile unit ($2\pi r_{cell}$). The result is that the force generation predicted for the outer hair cell is ~100 pN/mV. This coefficient agrees well with the experimental data of Adachi and Iwasa (1997) and Frank et al. (1999) for isolated outer hair cells and Xue et al. (1993) for cells in situ in the intact cochlea.

Effect of spectrin disruption

The membrane-bending model predicts that the equilibrium cell length, the passive stiffness of the cell, and, consequently, the force generation in unloaded cells will have contributions arising from the bending of the plasma membrane and from the extension of spectrin, because spectrin is represented as a spring in parallel with the membrane. Hence, the model predicts that disrupting spectrin will affect all these parameters. Experimentally, the spectrin network can be disrupted with diamide. The predicted magnitude of the reduction in passive force can be calculated by taking the ratio of the passive stiffness before and after the addition of diamide. The passive stiffness of the cell is proportional to the effective bending stiffness. If we consider k_{eff} to be the effective bending stiffness in a control cell and k_{effdia} to be the stiffness in the diamide-treated cell, then, for a

complete disruption of the spectrin network, the prediction is that

$$\frac{k_{\text{effdia}}}{k_{\text{eff}}} = \frac{k_c}{k_c + k_s n_{sp} b^2}. \tag{40}$$

Using our typical numbers of $k_c = 2 \times 10^{-19}$ J and $k_s = 1 \times 10^{-3}$ N/m, $k_{\text{effdia}}/k_{\text{eff}}$ is predicted to be 62%.

The active force generated by the cell is proportional to the passive stiffness. This is easily seen by rearranging Eq. 35 to read

$$f_o \mathcal{L}(\gamma(V - V_0)) = \frac{k_{\text{eff}}}{N_f b} (\Delta L_{\text{cell}} - \Delta L_{V0}). \tag{41}$$

In this equation, the left-hand side represents the active force, which is proportional to the effective spring constant. Adachi and Iwasa (1997) found that disrupting spectrin with diamide decreased the force generation in the cell in a concentration-dependent manner. The reduction in force generation ranged from 20 to 65% as the diamide concentration increased from 1 to 5 mM. Hence, the predictions of our model agree with the experimental observations. Our model also predicts that reducing the bending stiffness of the plasma membrane, which we postulate occurs on the application of salicylate (see Discussion), should also reduce the force generation in the cell, which has been experimentally shown (Hallworth, 1997).

For unloaded cells our model predicts that disruption of spectrin will change the resting length of the cell. If we assume that x_{dia} is the length of a diamide-treated cell and x_{con} is the resting length of a control cell, the relative change in cell length induced by diamide will be

$$\frac{x_{\text{dia}}}{x_{\text{con}}} = 1 - \frac{k_s n_{sp} b^2}{k_c + k_s n_{sp} b^2} \frac{x_o - a}{a}. \tag{42}$$

This equation predicts that the length of the diamide-treated cell will be shorter than the length of a control cell when $x_o > a$, i.e., when the initial length of spectrin is larger than the chord of the membrane arch. Likewise $x_{\text{dia}} > x_{\text{con}}$ when $x_o < a$. The latter is suggested by the sign of the bias term in the fit to the data of Santos-Sacchi (1992). From the fitted numerical value of ΔL_{V0}, we can estimate the force-free length of spectrin. If we assume that $c_i = 30$ nm, corresponding to $a = 40$ nm and $b = -2.2 \times 10^{-16}$ m^2, and that $k_{\text{eff}} = 4 \times 10^{-19}$ J and $n_{sp} = 2.5 \times 10^{15}$ m^{-2}, then the force-free length of spectrin is estimated to be approximately 39 nm.

DISCUSSION

We have proposed a new mechanism for outer hair cell electromotility. Active deformation of the outer hair cell occurs as a result of localized changes in the curvature of the plasma membrane. The curvature changes are driven by changes in the membrane polarization in accord with the flexoelectric formalism. This feature arises from the liquid-crystal character of the membrane. The mechanical force generated is sufficient to cause cell deformation. The Langevin function is able to predict the nonlinearity in the electromotility curve observed experimentally. The isometric force predicted in this model is consistent with experimental findings. This conclusion indicates that localized membrane bending is a plausible molecular mechanism for outer hair cell electromotility. Below, we consider how this model relates to other models of electromotility.

Coupling of the plasma membrane and the cytoskeleton

Researchers working on other cell types have discussed the idea of a connection between local bending of the plasma membrane and deformation in the cytoskeleton. In the red cell, it has been speculated that changes in the cytoskeletal proteins can result in local bending of the plasma membrane (Strey et al., 1995). In endothelial cells, Schmid-Schönbein et al. (1995) have analyzed the energy required to flatten the caveolae along the cell membrane and have related this to the cortical tension. Waugh (1996) has analyzed the energy required for bump formation on the surface of the red blood cell and included the effects of cytoskeletal deformation.

Our model of electromotility has proposed a motile unit in which membrane deformation and cytoskeletal deformation are intrinsically connected. Our prediction for the electromotility function (Eq. 35) and the force generation (Eq. 41) depend on both the bending stiffness of the membrane and the resistance of the cytoskeleton. In our picture, the active flexoelectric element must work against both passive stiffnesses because the elements are rigidly connected. Hence, our model predicts that agents that alter either the membrane (e.g., salicylate) or the cytoskeleton (e.g., diamide) will reduce force generation in the cell. The regularly spaced array of pillars provides the structural connection between the plasma membrane and the cytoskeleton. Electrically induced bending of the membrane between the pillars is the basis of our membrane-bending model of electromotility.

The membrane-bending model and the area-motor model

Previous models of outer hair cell electromotility have assumed the existence of motor molecules that change their conformation in response to a change in membrane potential (Iwasa, 1994; Dallos et al., 1993; Santos-Sacchi, 1993). The conformational change is in the plane of the membrane and often explicitly stated to be an area change (Iwasa, 1996; Kalinec et al., 1992; Holley, 1996; Santos-Sacchi, 1993), hence, we refer to these models as "area-motor" models.

The motor molecules are assumed to exist in only two states: an extended state and a compact state. The probability of a motor being in either state is described by a Boltzmann distribution and is a function of membrane potential. When the membrane potential changes, the motor molecule changes its area. Although the exact location of the motor is not specified, it is often assumed to be in the plasma membrane (Santos-Sacchi, 1993; Holley, 1996; Iwasa, 1994; Kalinec et al., 1992; Gale and Ashmore, 1997a,b). The observation from freeze fracture microscopy that the plasma membrane possesses a high density of intramembraneous particles (Gulley and Reese, 1977; Forge, 1991) led to the view that conformational changes in these particles (presumably proteins) were responsible for the motility of the cell. Several investigators have suggested that these plasmalemmal particles observed in electron micrographs are, in fact, the motor molecules that change their area (Kalinec et al., 1992; Holley, 1996; Iwasa, 1994; Huang and Santos-Sacchi, 1994).

The area-motor models successfully predict the nonlinear features of voltage-dependent motility. The experimental data can be adequately fit to Boltzmann functions, and reasonable values are obtained for the free parameters (number of motor molecules and charge per motor). The area-motor models rationalize the existence of the intramembraneous particles. They explain why motility remains after digestion of intracellular structures with trypsin (Kalinec et al., 1992). The observations that movement can be detected in a patch of membrane attached to the cell (Kalinec et al., 1992) and that movement can be detected in an excised patch of membrane (Gale and Ashmore, 1997a) are also explained by the area-motor model. Hence, the area-motor model has predictive power and also explains qualitative cell features associated with motility.

However, there are some features of electromotility not explained by the area-motor hypothesis. First, there is no compelling evidence that area changes actually occur in the plasma membrane during electromotility. One issue that has been raised is that the linear capacitance of the membrane appears to remain constant during electromotility and during osmotically induced changes in cell length (Iwasa, 1996; Adachi and Iwasa, 1998). Although there may be several explanations for this result, including sensitivity of experimental techniques, one possible explanation is that actual area changes do not occur, but rather, cell length changes involve unraveling of the folds in the membrane (Iwasa, 1996). Second, it has recently been demonstrated that the density of intramembraneous particles does not correspond to the number of voltage sensors (Santos-Sacchi et al., 1998). In fact, in short cells, the charge density can even exceed the theoretical maximal limit for packing 10 nm particles. This means that either the Boltzmann description is inadequate or that the membrane particles are not the voltage sensors.

Evidence indicating a role for membrane curvature

Support for a role for membrane curvature in outer hair cell electromotility comes from several experimental observations. As already noted, transmission electron micrographs of the outer hair cell do not reveal a smooth plasma membrane, but a folded one (Saito, 1983; Dieler et al., 1991). Ulfendahl and Slepecky (1988) presented evidence that cell shortening induced by potassium depolarization increased the rippling of the plasma membrane. Recent measurements indicate that the lateral diffusion of fluorescent probes in the plasma membrane of the outer hair cell is sensitive to voltage- and tension-induced changes in cell length and also to curvature reagents (Oghalai et al., 2000). These results can be interpreted in terms of changes in the nanoscale rippling of the plasma membrane during these manipulations. In other experiments in which the intracellular structures are digested with trypsin, the normal folding of the membrane is disrupted. However, such membranes still appear to possess local regions of curvature, as shown in the electron micrographs of Huang and Santos-Sacchi (1994). This suggests the membrane may possess spontaneous curvature. Micropipette experiments reveal that it is possible to pull off a large number of vesicles from an aspirated outer hair cell (Sit et al., 1997). This implies the presence of excess area in the plasma membrane of the outer hair cell. Recent quantitative estimates indicate that the first few vesicles are probably due to an unraveling of the ripples (Morimoto et al., 2000). This concept, that the outer hair cell possesses excess area stored in the form of high curvature folds, is not unique to outer hair cells, but appears to be an almost ubiquitous occurrence, because it is found in other cell types such as endothelial cells, leukocytes, red blood cells, and smooth muscle cells (Schmid-Schönbein et al., 1995).

All experimental evidence indicates that the outer hair cell membrane is in the fluid-lamellar state. We have recently measured the diffusion coefficient of fluorescent lipid probes in the membrane and demonstrated that it falls within the range expected for a fluid phase membrane (Oghalai et al., 1999). Moreover, Santos-Sacchi and Zhao (1999) obtained evidence that the outer hair cell voltage sensors may diffuse in the membrane. Consequently, any micromechanical model of the outer hair cell must be consistent with the well-established fact that biological membranes in the fluid-lamellar state are soft yet essentially incompressible surfaces (Bloom et al., 1991). They have a large resistance to changes in their area, but bend quite easily. Although significant electrically induced changes in membrane area are conceivable, they do not seem to be a general occurrence in biology and are likely to be more energetically costly than curvature changes. In contrast, electrically induced changes in membrane curvature are well-studied phenomena. Indeed, shape transformations of

vesicles and red blood cells consistent with changes in membrane curvature are observed on the application of electric fields (Meleard et al., 1998).

Additional support for the membrane-bending model comes from the observation that well-known inhibitors of electromotility, salicylate and the lanthanide ions, are also agents that will affect the ability of the membrane to bend. The $K_{1/2}$ for salicylate diminishment of the nonlinear capacitance has been reported to be 1.6 mM with a maximal dose being 10 mM (Kakehata and Santos-Sacchi, 1996). Such a high concentration may be explained in two ways. First, it is possible that salicylate is exerting a general effect on the membrane as opposed to a specific effect on a protein. Second, it is possible that salicylate is acting at an intracellular site at a lower concentration than the external concentration. In the whole-cell recording mode, salicylate is capable of diminishing the nonlinear capacitance regardless of whether it is applied externally or internally (Kakehata and Santos-Sacchi, 1996). We have recently verified this in cell attached and excised patches (Raphael et al., 1998). If salicylate does incorporate into one leaflet of the membrane, it will alter membrane curvature stress. Interestingly, in red blood cells, salicylate partitions into the outer leaflet of the membrane and causes an echinocytic shape transformation (Reinhart et al., 1988). We have recently shown that salicylate decreases the area compressibility modulus (and therefore the bending stiffness) in pure synthetic vesicles (Raphael et al., 1999). This observation suggests that salicylate may act in the outer hair cell by reducing its bending stiffness. A softer membrane would be less effective at converting electrical energy derived at the plasma membrane to the cytoskeleton (See Eq. 10). As a result, motility would be diminished, but not totally inhibited. Alternatively, the presence of a charged salicylate molecule in the membrane could interact with the voltage sensor and alter the effective dipole moment. A reduction in the dipole moment could lead to an apparent linear electromotility curve, as shown in Fig. 9 (cf. with Fig. 6 in Kakehata and Santos-Sacchi, 1996). Lanthanide ions, such as gadolinium, screen surface charges and would inhibit any flexoelectric type of response. In this context, Santos-Sacchi's observation of "depolarization-induced membrane dimpling" in deflated cells, which was sensitive to gadolinium (Santos-Sacchi, 1991), could be interpreted in light of the membrane-bending model.

Comparison of force required for membrane bending versus membrane expansion

The force required for membrane bending is much lower than the force required for membrane area change. To illustrate this in our outer hair cell model, let us suppose that the membrane is flat between the pillars and must expand in plane when the cell length increases. In this case, the force per unit length, or tension generated in the membrane, is given by

$$\tau = \frac{\partial \tilde{U}}{\partial \alpha} = K\alpha = K\frac{R_2L_2 - R_1L_1}{R_1L_1}. \qquad (43)$$

Let us use the same parameters we used in our simulation of membrane bending: an interpillar distance of $L_1 = 40$ nm, which extends to $L_2 = 40.1$ nm during cell elongation. If we assume constant volume, then $R_2 = R_1(L_1/L_2)^{1/2}$, and the fractional area change will be 0.12%. For the plasma membrane, Adachi and Iwasa (1999) estimated $K = 130$ mN/m in an outer hair cell in which the intracellular structures were digested with trypsin (which corresponds to a bending stiffness of 2.7×10^{-19} J using Eq. 10). By Eq. 43, the tension required to extend the membrane sheet will be 1.6×10^{-4} N/m. In contrast, we previously estimated that the force per unit length required to bend the membrane will be 4×10^{-6} N/m. This analysis shows that the membrane-bending mechanism is more efficient (requires less energy for the same deformation) than the area expansion mechanism. This conclusion remains true even if the bending rigidity of the plasma membrane is an order of magnitude higher than it is for a red blood cell or a lipid vesicle packed with cholesterol.

The Langevin function description: molecular orientation of the motor in the membrane

The membrane-bending model differs from the area-motor models in the function used to describe the nonlinearity of the electromotile response. The bending model is based upon electric dipoles in the membrane. When an external electric field is applied, these dipoles rotate to line up in the direction of the field. The fraction of dipoles aligned in the direction of the field is described by the Langevin function. The Langevin function is derived from statistical mechanics (see Appendix B), but provides for a continuous distribution of molecular states. Hence, our picture differs from the picture that each molecule possesses only two states and that the probability of being in one of these states is determined by the voltage in accord with the Boltzmann distribution. Rather, our model assumes that each molecule can be in any number of orientations. As the external field is increased, the probability that a molecule will be aligned in the direction of the field increases until all the molecules align with the field and saturation is reached. The Langevin function has previously been shown to be capable of fitting outer hair cell electromotility data, where the effects on the estimated charge per voltage sensor were discussed (Huang and Santos-Sacchi, 1993). Below, we discuss the results of our fit of the Langevin function in terms of the molecular dipole moment.

The Langevin function becomes nonlinear when its argument ξ approaches 2. The function saturates very slowly,

because saturation is not reached until the argument becomes greater than 5. It is worthwhile to discuss the physical implications of this. Lipid molecules can have a dipole moment of up to 10 Debye (Petrov, 1999). (1 Debye = 1 D = 3.333×10^{-30} C m). This implies that nonlinearity will become apparent when the polarizing field E_p reaches 2.5×10^8 V/m, and saturation will be approached when the polarizing field reaches 6×10^8 V/m. Protein molecules can possess large regions of charge separation and can have dipole moments on the order of several hundred Debye (Takashima, 1999). For a protein molecule with a dipole moment of 100 D, nonlinearity will set in when the polarizing field reaches 2.5×10^7 V/m and saturation will be approached when the polarizing field reaches 6×10^7 V/m, as illustrated in Fig. 8. The relationship between the polarizing field and the external field depends on the magnitude of the dipole moment and the number of dipoles and is derived in Appendix B. If the dipole density corresponds to the density of intramembraneous particles, $6000/\mu m^2$, and $p_o = 125$ D, a polarizing field of 1×10^8 V/m will correspond to a transmembrane potential of 181 mV. Alternatively, if the dipole density corresponds to $16{,}000/\mu m^2$ and $p_o = 50$ D, then a polarizing field of 1×10^8 V/m will be equivalent to 372 mV. Note that $p_o = 50$ D corresponds to about one electronic charge separated by the distance across the membrane (5 nm).

The fit to the experimental data in Fig. 9 yielded a value for the parameter γ of 0.09 mV^{-1}. Combining Eq. 36 and Eq. B8 in Appendix B, yields an expression for solving for the dipole moment p_o in terms of the dipole density N. If the dipole density is $6000/\mu m^2$, the model predicts that $p_o = 136$ D. In contrast, if the dipole density corresponds to the density of lipids in the membrane, $2 \times 10^6/\mu m^2$, then $p_o = 8.5$ D. Hence, the data do not allow us to differentiate whether the dipoles in the membrane are associated with the particles or with the surrounding lipids, or both. The data are fit equally well by permanent dipoles in the membrane corresponding to the density of the particles possessing a dipole moment similar to that of membrane proteins or by permanent dipoles corresponding to the density of membrane lipids, which possess a dipole moment consistent with lipids. We discuss the physical implication of these estimates below.

Possible mechanisms for electrically induced curvature changes

We have presented a model for electromotility that assumes that localized curvature changes occur in the membrane as a result of a variation in the transmembrane potential. The model is presented in the phenomenological framework of flexoelectricity, and we postulate that the molecular mechanism is change of orientation of dipoles in the membrane. However, we have not stated whether the dipoles are associated with protein or lipid molecules, which are two alternative but not mutually exclusive possibilities.

Our model is consistent with a protein conformational change along the lines postulated by the area-motor model. However, we postulate that the result of this conformational change may be to change the curvature of the membrane, while leaving its surface area constant. One possibility is that electric fields could induce aggregation of membrane proteins. Theoretical models predict that protein aggregation can lead to curvature deformation (Kim et al., 1998). Another possibility is that voltage-dependent insertion of amino acid side chains occurs, which expands one leaflet of the bilayer relative to the other leaflet and leads to curvature deformation.

However, the lack of sensitivity of outer hair cell electromotility to protein-specific reagents (Frolenkov et al., 1998) leads us to the consideration that perhaps the lipid component of the bilayer could play a significant role in the molecular mechanism of electromotility. Electric fields can induce shape transformations in pure lipid membranes by inducing a change in the curvature of the membrane (Helfrich, 1974; Sokirko et al., 1994). Molecular models of flexoelectricity relate the flexoelectric coefficient f to the lipid dipole moment (Todorov et al., 1994a) and to the shift in the surface charge equilibrium that occurs when the membrane bends (Petrov and Sokolov, 1986).

Hence, our model allows for dipole moments associated with both protein and lipids to contribute to electromotility. One possible scenario is that a protein conformational change causes (is accompanied by) the bending of the membrane. Under such a scheme, there would then be a specific capacitance associated with the protein conformational change and a nonspecific capacitance associated with the electrically induced flexion of the membrane. The recent report of Santos-Sacchi and Wu (1998) that both protein and lipid reagents affect the nonlinear capacitance to some degree would support such an interpretation.

Flexoelectricity and piezoelectricity

We emphasize that, although the piezoelectric and the flexoelectric formalisms are similar, the underlying physical processes are different. As one author wrote, the flexoelectric effect "is not identical with the piezoelectric effect of solid crystals where a charge arises on the surface by compression or dilation. Because, in the case of the nematic liquid crystal, the physical origin is not translational deformations, as in solids, but rather curvature strains (orientation deformation)" (Pelzl, 1994). In his classic work on liquid crystals, Chandrasekhar (1992) also discusses the flexoelectric effect as being an inherent property of all nematic liquid crystals. When the point is made that liquid crystals exhibit flexoelectricity and not piezoelectricity, and that biological membranes are liquid crystals, we are led to hypothesize that the membrane-based motility in the outer hair cell is flexoelectric. However, the projection of a curvature change in the plane of the membrane will appear as an apparent area change, and

thus a nanoscale flexoelectric mechanism can be phenomenologically described in terms of a piezoelectric model.

Flexoelectricity as a mechanism for high frequency force production

The mechanism of outer hair cell electromotility must satisfy the challenging requirement of maintaining its efficiency even at high frequencies. It was recently shown that the force production in the outer hair cell is independent of frequency up to at least 50 kHz (Frank et al., 1999). The voltage-dependent movements observed by Mosbacher et al. (1998) revealed a possible flexoelectric mechanism independent of frequency. Flexoelectricity is very effective as a high-frequency electromechanical transduction mechanism because it is able to provide increasing currents with increasing stimulus frequency (Petrov and Usherwood, 1994). The electromechanical coupling coefficient for flexoelectricity is much higher than for piezoelectricity due to the low value of the bending stiffness compared to the area expansion modulus. Indeed, the coupling coefficient for flexoelectricity could approach the value of 1, whereas, for membrane piezoelectricity, it is estimated to be on the order of 10^{-4} (Petrov and Usherwood, 1994). Additionally, a lipid-based mechanism would be intrinsically faster than a protein-based mechanism, because the time for the rotation of a lipid dipole in the membrane is faster than that for a large protein undergoing conformational changes.

Proposed experimental validation of the model

The model presented in this paper motivates a new experimental line of investigation not considered under the area-motor paradigm. First, it should be substantiated that nanoscale curvature changes occur in the outer hair cell during cell length changes. This involves the use of sensitive techniques for looking at surfaces of biological membranes. One approach would be to use polarized total internal reflection microscopy, which has been shown to be capable of resolving curvature changes in membranes not visible with the light microscope (Sund et al., 1999). Another approach would be to use atomic force microscopy to map the surface of the membrane at different membrane potentials. If the sensitivity of these techniques is sufficiently adequate, and they fail to detect curvature changes, this could disprove the proposed flexoelectric model. Other experiments motivated by this model are to examine the effect of pharmacological reagents that change membrane curvature on the nonlinear capacitance and electromotility of the outer hair cell.

CONCLUSION

In this work, we have presented a membrane-bending model of outer hair cell electromotility. This is a novel mechanism for outer hair cell electromotility yet is rooted in well-known liquid crystal physics of phospholipid membranes and the electrically induced deformations associated with liquid crystals. This is the first model of hair cell motility that postulates that out-of-plane bending deformations can function as an active motor and is consistent with constant surface area during electromotility. Although we have demonstrated its feasibility for electromechanical transduction, the ability of the constitutive equations to describe the properties of the outer hair cell, such as nonlinear capacitance and the effect of turgor pressure, needs further development. However, a flexoelectric mechanism will enable high-frequency force generation and is a candidate for the molecular basis of the elusive yet essential electromechanical transduction that makes human hearing possible.

APPENDIX A

We assume that the contour of the membrane between the points of attachment to the pillar can be described as following the arc of a circle. In other words, the membrane can be described as a smooth surface with an arc length of

$$s = R \cdot 2\theta, \tag{A1}$$

where R is the radius of curvature of the surface. This geometry is illustrated in Fig. 3. It is postulated that the curved element deforms in such a way that its arc length remains constant (equivalent to the assumption of a constant surface area in the two-dimensional case). Let us assume that all of the extensile work produced by bending goes into extension of the spring. How far will the spring extend in this case?

We assume that, under extensile deformation, the surface remains smooth and can be parameterized by the same equation as above, though with a larger radius of curvature. The relationship between the spring length and the membrane curvature is

$$x = 2R \sin\theta = \frac{2}{c} \sin\frac{sc}{2}, \tag{A2}$$

where $c = 1/R$. Hence, the relationship between the spring length and the curvature is nonlinear. For small deformations, we linearize the function $x(c)$ about an initial curvature, which we designate c_i. The function then takes the form,

$$x(c) = \frac{2}{c_i} \sin\frac{sc_i}{2} + (c - c_i)\left(\frac{s}{c_i}\cos\frac{sc_i}{2} - \frac{2}{c_i^2}\sin\frac{sc_i}{2}\right). \tag{A3}$$

We note that, if $c_i = 0$ (corresponding to a flat membrane), then when $c \to 0$, $x \to s$, which is a trivial result. Hence, we consider the situations where the membrane is initially curved. The initial curvature c_i may be set by the spontaneous curvature or by other forces such as the turgor pressure in the cell. The above equation can be expressed in a more convenient form as

$$x(c) = a + b(c - c_i) \tag{A4}$$

$$\text{where} \quad a = \frac{2}{c_i}\sin\frac{sc_i}{2}$$

$$b = \frac{s}{c_i}\cos\frac{sc_i}{2} - \frac{2}{c_i^2}\sin\frac{sc_i}{2},$$

where a will have units of length (m) and b will have units of m^2. Using this substitution, the expression for the internal energy (Eq. 6) is written as

$$\tilde{U}_m = \tfrac{1}{2} k_c(c - c_o)^2 + \tfrac{1}{2} k_s n_{sp}[a + b(c - c_i) - x_o)]^2, \quad \text{(A5)}$$

where we have only written the contributions in the longitudinal direction and have neglected the second radius of curvature.

At equilibrium, the partial derivative of the internal energy is equal to zero. We can calculate the equilibrium curvature in terms of the elastic constants for bending and extension, the resting spring length, and the spontaneous curvature as

$$\frac{\partial \tilde{U}}{\partial c} = 0 = k_c(c_l - c_o) + k_s n_{sp}(b(c_l - c_i) + a - x_o)b. \quad \text{(A6)}$$

If we now identify the spontaneous curvature with the initial curvature, $c_o = c_i$, an expression for the equilibrium curvature in the longitudinal direction, $c_l = c_e$, can be written as

$$c_e = c_o - \frac{k_s n_{sp} b(a - x_o)}{k_c + k_s n_{sp} b^2}. \quad \text{(A7)}$$

The internal energy can then be written in terms of the equilibrium curvature as

$$\tilde{U}_m = \tfrac{1}{2} k_{eff}(c - c_e)^2 + G \quad \text{(A8)}$$

where

$$k_{eff} \equiv k_c + k_s n_{sp} b^2,$$

$$G \equiv \tfrac{1}{2} k_s(a^2 - 2ax_o + x_o^2) + \left(\frac{(x_o - a)bk_s}{k_{eff}}\right)^2.$$

Note that k_{eff} appears as an effective bending stiffness and G as a constant, depending on the initial configuration of the membrane-spring system.

APPENDIX B

The Langevin function

For a molecular dipole with permanent moment p_o residing in a polarizing field E_p, the interaction energy between the dipole and the field is given as

$$U_D = p_o E_p \cos\theta, \quad \text{(B1)}$$

where θ is the angle the dipole moment makes with the field. A collection of dipoles will exist in any number of orientations respective to the field. Statistical mechanics predicts that the number of molecules with their dipole axes falling within the solid angle $d\Omega = 2\pi \sin\theta\, d\theta$ is

$$A_n \exp(-U_D/kT)d\Omega = A_n \exp -(p_o E_p/kT)\cos\theta)d\Omega, \quad \text{(B2)}$$

where A_n is a constant that depends on the number of molecules. The total number of molecules is obtained from integration over all possible directions. The total dipole moment in the direction of the field is simply the dipole moment of each molecule in the direction of the field multiplied by the total number of molecules aligned in the direction of the field:

$$\int A_n \exp(-(p_o E_p/kT)\cos\theta)p_o \cos\theta\, d\Omega. \quad \text{(B3)}$$

The ratio of the average component in the direction of the field to the permanent moment is

$$\frac{\langle p_o \cos\theta\rangle}{p_o} = \frac{\int \exp(-(p_o E_p/kT)\cos\theta)\cos\theta\, d\Omega}{\int \exp(-(p_o E_p/kT)\cos\theta) d\Omega} = \mathcal{L}(\xi). \quad \text{(B4)}$$

When this equation is integrated, the right-hand side is the Langevin function.

Relationship between local field and externally applied field

The Langevin function is expressed in terms of the local or polarizing field E_p. This field can be related to the external field by the relationship (Reitz and Milford, 1960)

$$E_p = E + \frac{P}{3\varepsilon_o}, \quad \text{(B5)}$$

where P is the polarization per unit volume ($P_s = Ph$). This relationship was derived by Lorentz and is valid when all the dipoles around the dipole in question are distributed isotropically. The outer hair cell membrane is, of course, fluid and the dipoles are free to change their position. However, there is a high density of dipoles in the membrane, and this will give the structure a time-averaged order. Hence, we believe this relationship is justified for the outer hair cell because the average position of the dipoles in the membrane remains constant on the time scale of interest. Substituting the expression for the Langevin function for P yields

$$E_p = E + \frac{N p_o \mathcal{L}(\xi)}{3h\varepsilon_o}. \quad \text{(B6)}$$

In the linear region, the Langevin can be linearized ($\mathcal{L}(\xi) = \xi/3$). The above relationship can be written as

$$E_p = E + \frac{N p_o^2 E_p}{9h\varepsilon_o kT} \quad \text{(B7)}$$

or

$$E = E_p(1 - \lambda) \quad \text{where} \quad \lambda = \frac{N p_o^2}{9h\varepsilon_o kT}. \quad \text{(B8)}$$

Hence, when $\lambda \ll 1$, the external field is equal to the polarizing field. When the number of dipoles becomes large and the dipole moment of each molecule is larger, λ approaches 1. In this case, the external electric field is much smaller than the polarizing field. To relate E to E_p, we must know N and p_o. For the outer hair cell, if we assume a dipole density of $6000/\mu m^2$ and $p_o = 125$ D, we calculate that $\lambda \approx 0.63$, and a polarizing field of 1×10^8 V/m will correspond to a transmembrane potential of 180 mV.

The authors are grateful for stimulating discussions with Richard Waugh, Vinod Sharma, Charles Eggleton, Kathleen Stebe, Alexander Spector, Tilak Ratnanather, John Halter, Takashi Nakagawa, and John Oghalai.

This work was supported by National Institutes of Health grants DC02775, DC00354, DC00979, and NRSA DC00363.

REFERENCES

Adachi, M. and K. H. Iwasa. 1997. Effect of diamide on force generation and axial stiffness of the cochlear outer hair cell. *Biophys. J.* 73: 2809–2818.

Adachi, M. and K. H. Iwasa. 1998. Pressure insensitivity of outer hair motility. *Biophys. J.* 74:A86.

Adachi, M. and K. H. Iwasa. 1999. Electrically driven motor in the outer hair cell: effect of a mechanical constraint. *Proc. Natl. Acad. Sci. USA.* 96:7244–7249.

Ashmore, J. F. 1994. The cellular machinery of the cochlea. *Exp. Physiol.* 79:113–134.

Ashmore, J. F. 1987. A fast motile response in guinea-pig outer hair cells: The cellular basis of the cochlea amplifier. *J. Physiol.* 388:323–347.

Bloom, M., E. A. Evans, and O. Mouritsen. 1991. Physical properties of the fluid lipid-bilayer component of cell membranes: a perspective. *Quart. Rev. Biophys.* 24:293–397.

Boey, S. K., D. H. Beal, and D. E. Discher. 1998. Simulations of erythrocyte cytoskeleton at large deformation. I. Microscopic models. *Biophys. J.* 75:1573–1583.

Brownell, W. E., C. R. Bader, D. Bertrand, and Y. de Ribaupierre. 1985. Evoked mechanical responses of isolated cochlear outer hair cells. *Science.* 227:194–196.

Brownell, W. E. and A. S. Popel. 1998. Electrical and mechanical anatomy of the outer hair cell. *In* Psychophysical and Physiological Advances in Hearing. A. R. Palmer, A. Rees, A. Q. Summerfield and R. Meddis, editors. Whurr Publishers Ltd, London, 89–96.

Cady, W. G. 1946. Piezoelectricity. McGraw-Hill Book Co., New York.

Chandrasekhar, S. 1992. Liquid Crystals. Cambridge University Press, Cambridge, U.K. 205–211.

Collings, P. J. 1990. Liquid Crystals. Princeton University Press, Princeton, NJ.

Dallos, P. 1997. Outer hair cells: the inside story. *Ann. Otol. Rhinol. Laryngol.* 106:16–22.

Dallos, P., B. N. Evans, and R. Hallworth. 1991. Nature of the motor element in electrokinetic shape changes of cochlear outer hair cells. *Nature.* 350:155–157.

Dallos, P., R. Hallworth, and B. N. Evans. 1993. Theory of electrically driven shape changes of cochlear outer hair cells. *J. Neurophys.* 70: 299–323.

De Gennes, 1974. The Physics of Liquid Crystals. Clarendon Press, Oxford, U.K.

Derzhanski, A., A. G. Petrov, A. T. Todorov, and K. Hristova. 1990. Flexoelectricity of lipid bilayers. *Liquid Crystals.* 7:439–449.

Dieler, R., W. Shehata-Dieler, and W. E. Brownell. 1991. Concomitant salicylate-induced alterations of outer hair cell subsurface cisternae and electromotility. *J. Neurocytol.* 20:637–653.

Evans, E. A. 1974. Bending moments and chemically induced moments in membrane bilayers. *Biophys. J.* 16:13–26.

Evans, E. A. and R. Skalak. 1980. Mechanics and Thermodynamics of Biomembranes. CRC Press Inc., Boca Raton, FL.

Frank, G., W. Hemmert, and A. W. Gummer. 1999. Limiting dynamics of high-frequency electromechanical transduction of outer hair cells. *Proc. Natl. Acad. Sci. USA.* 96:4420–4425.

Frolenkov, G. I., M. Atzori, F. Kalinec, F. Mammano, and B. Kachar. 1998. The membrane-based mechanism of cell motility in cochlear outer hair cells. *Mol. Biol. Cell.* 9:1961–1968.

Furness, D. N. and C. M. Hackney. 1990. Comparative ultrastructure of subsurface cisternae in inner and outer hair cells of the guinea pig cochlea. *Eur. Arch. Otol. Rhinol. Laryngol.* 247:12–15.

Forge, A. 1991. Structural features of the lateral walls in mammalian cochlear outer hair cells. *Cell & Tissue Res.* 265:473–483.

Gale, J. E. and J. F. Ashmore. 1997a. An intrinsic frequency limit to the cochlear amplifier. *Nature.* 389:63–66.

Gale, J. E. and J. F. Ashmore. 1997b. The outer hair cell motor in membrane patches. *Pflugers Arch.* 434:267–271.

Gulley, R. L. and T. S. Reese. 1977. Regional specialization of the hair cell plasmalemma in the organ of corti. *Anat. Rec.* 189:109–124.

Hallworth, R. 1997. Modulation of outer hair cell compliance and force by agents that affect hearing. *Hear. Res.* 114:204–212.

Hansen, J. C., R. Skalak, S. Chien, and A. Hoger. 1996. An elastic network model based on the structure of the red blood cell membrane skeleton. *Biophys. J.* 70:146–166.

Helfrich, W. 1973. Elastic properties of lipid bilayers: theory and possible experiments. *Z. Naturforsch.* 28:693–703.

Helfrich, W. 1974. Deformation of lipid bilayer spheres by electric field. *Z. Naturforsch.* 29:510–515.

Holley, M. C. 1996. Outer hair cell motility. *In* The Cochlea. P. Dallos, A. N. Popper, R. R. Fay, editors. Springer-Verlag, New York. 386–434.

Holley, M. C., F. Kalinec, and B. Kachar. 1992. Structure of the cortical cytoskeleton in mammalian outer hair cells. *J. Cell Sci.* 102:569–580.

Hristova, K., I. Bivas, A. G. Petrov, and A. Derzhanski. 1991. Influence of the electric double layers of the membrane on the value of its flexoelectric coefficient. *Mol. Crys. Liq. Cryst.* 200:71–77.

Huang, G. and J. Santos-Sacchi. 1993. Mapping the distribution of outer hair cell motility voltage sensor by electrical amputation. *Biophys. J.* 65:2228–2236.

Huang, G. and J. Santos-Sacchi. 1994. Motility voltage sensor of the outer hair cell resides within the lateral plasma membrane. *Proc. Natl. Acad. Sci. USA.* 91:12268–12272.

Hwang, W. C. and R. E. Waugh. 1997. Energy of disassociation of lipid bilayer from the membrane skeleton of red blood cells. *Biophys. J.* 72:2669–2678.

Iwasa, K. H. 1994. A membrane motor model for the fast motility of the outer hair cell. *J. Acoust. Soc. Am.* 96:2216–2224.

Iwasa, K. H. 1996. Membrane motor in the outer hair cell of the mammalian ear. *Comments Theor. Biol.* 4:93–114.

Kakehata, S. and J. Santos-Sacchi. 1996. Effects of salicylate and lanthanides on outer hair cell motility and associated gating charge. *J. Neurosci.* 16:4881–4889.

Kalinec, F., M. C. Holley, K. H. Iwasa, D. J. Lim, and B. Kachar. 1992. A membrane-based force generation mechanism in auditory sensory cells. *Proc. Natl. Acad. Sci. USA.* 89:8671–8675.

Kim, K. S., J. Neu, and G. Oster. 1998. Curvature-mediated interactions between membrane proteins. *Biophys. J.* 75:2274–2291.

Kubisch, C., B. C. Schroeder, T. Friedrich, B. Lutjohann, A. El-Amraoui, S. Marlin, C. Petit, and T. J. Jentsch. 1999. KCNQ4, a novel potassium channel expressed in sensory outer hair cells, is mutated in dominant deafness. *Cell.* 96:437–446.

Lim, D. J. and F. Kalinec. 1998. Cell and molecular basis of hearing. *Kidney Int.* 53:S104–S113.

Lines, M. E. and A. M. Glass. 1977. Principles and Applications of Ferroelectrics and Related Materials. Clarendon Press, Oxford, U.K. 57–71.

Meleard, P., G. Gerbeaud, P. Bardusco, N. Jeandaine, M. D. Mitov, and L. Fernandez-Puente. 1998. Mechanical properties of model membranes studied from shape-transformations of giant vesicles. *Biochimie.* 80: 401–413.

Meyer, R. B. 1969. Piezoelectric effects in liquid crystals. *Phys. Rev. Lett.* 22:918–921.

Mosbacher, J., M. Langer, J. K. H. Horber, and F. Sachs. 1998. Voltage-dependent membrane displacements measured by atomic force microscopy. *J. Gen. Physiol.* 111:65–74.

Morimoto, N., A. Nygren, and W. E. Brownell. 2000. Quantitative assessment of drug-induced changes in OHC lateral wall mechanics. *In* Recent Developments in Auditory Mechanics. H. Wada and T. Takasaka, editors. World Scientific Publishing Co. Pte. Ltd., Taipei, Taiwan. 261–267.

Mountain, D. C., and A. E. Hubbard. 1994. A piezoelectric model of outer hair cell function. *J. Acoust. Soc. Am.* 95:350–354.

Nobili, R., F. Mammano, and J. F. Ashmore. 1998. How well do we understand the cochlea? *Trends Neurosci.* 21:159–167.

Oghalai, J. S., A. A. Patel, T. Nakagawa, and W. E. Brownell. 1998. Fluorescence-imaged microdeformation of the outer hair cell lateral wall. *J. Neurosci.* 18:48–58.

Oghalai, J. S., T. D. Tran, R. M. Raphael, T. Nakagawa, and W. E. Brownell. 1999. Transverse and lateral mobility in outer hair cell lateral wall membranes. *Hear. Res.* 135:19–28.

Oghalai, J. S., H. B. Zhao, J. W. Kutz, and W. E. Brownell. 2000. Voltage and tension regulate lipid mobility in the outer hair cell plasma membrane. *Science.* 287:658–661.

Pelzl, G. 1994. Thermodynamic behavior and physical properties of thermotropic liquid crystals. *In* Liquid Crystals. H. Stegmeyer, guest editor, Springer, New York.

Petrov, A. G. 1975. Flexoelectric model for active transport. *In* Physical and Chemical Basis of Biological Information Transfer. Plenum Press, New York. 111–125.

Petrov, A. G. 1999. The Lyotropic State of Matter: Molecular Physics and Living Matter Physics. Gordon and Breach Science Publishers, Amsterdam, The Netherlands.

Petrov, A. G. and P. N. R. Usherwood. 1994. Mechanosensitivity of cell membranes. *Eur. Biophys. J.* 23:1–19.

Petrov, A. G. and V. S. Sokolov. 1986. Curvature-electric effect in black lipid membranes. *Eur. Biophys. J.* 13:139–155.

Raphael, R. M. and R. E. Waugh. 1996. Accelerated interleaflet transport of phosphatidylcholine molecules in membranes under deformation. *Biophys. J.* 71:1374–1388.

Raphael, R. M., T. Nakagawa, A. S. Popel, and W. E. Brownell. 1998. High resolution recordings of the outer hair cell voltage sensor. *Assoc. Res. Otolaryngol. Abs.* 21:17.

Raphael, R. M., T. Nguyen, and A. S. Popel. 1999. Salicylate induced softening of membrane bilayers. *Biophys. J.* 76:A273.

Reinhart, W. H., L. P. Sung, K. L. Sung, S. Bernstein, and S. Chien. 1988. Impaired echinocytic transformation of ankyrin- and spectrin-deficient erythrocytes in mice. *Am. J. Hematol.* 29:195–200.

Reitz, J. R. and F. J. Milford. 1960. Foundations of Electromagnetic Theory. Addison-Wesley, Inc. Reading, Mass. 93–101.

Saito, K. 1983. Fine structure of the sensory epithelium of guinea-pig organ of Corti: subsurface cisternae and lamellar bodies in the outer hair cells. *Cell & Tissue Res.* 229:467–481.

Santos-Sacchi, J. 1991. Reversible inhibition of voltage-dependent outer hair cell motility and capacitance. *J. Neurosci.* 10:3096–3110.

Santos-Sacchi, J. 1992. On the frequency limit and phase of outer hair cell motility: effects of the membrane filter. *J. Neurosci.* 12:1906–1916.

Santos-Sacchi, J. 1993. Harmonics of outer hair cell motility. *Biophys. J.* 65:2217–2227.

Santos-Sacchi, J. and M. Wu. 1998. Electrical correlates of OHC viscoelastic behaviour—evidence for voltage induced membrane tension. *Assoc. Res. Otolaryngol. Abs.* 21:63.

Santos-Sacchi, J. and H. B. Zhao. 1999. Green card motors: OHC lateral membrane molecular motors may travel. *Assoc. Res. Otolaryngol. Abs.* 22.

Santos-Sacchi, J., S. Kakehata, T. Kikuchi, Y. Katori, and T. Takasaka. 1998. Density of motility-related charge in the outer hair cell of the guinea pig is related to best frequency. *Neurosci. Lett.* 256:155–158.

Servuss, R. M., W. Harbich, and W. Helfrich. 1976. Measurement of the curvature elastic modulus of egg lecithin bilayers. *Biochim. Biophys. Acta.* 436:900–903.

Schmid-Schönbein, G. W., T. Kosawada, R. Skalak, and S. Chien. 1995. Membrane model of endothelial cells and leukocytes. A proposal for the origin of a cortical stress. *J. Biomech. Eng.* 117:171–178.

Schneider, M. B., J. T. Jenkins, and W. W. Webb. 1984. Thermal fluctuations of large cylindrical phospholipid vesicles. *Biophys. J.* 45: 891–899.

Sit, P. S., A. A. Spector, A. Lue, A. S. Popel, and W. E. Brownell. 1997. Micropipet aspiration on the outer hair cell lateral wall. *Biophys. J.* 72:2812–2819.

Smith, C. A. 1968. Ultrastructure of the organ of Corti. *Adv. Sci.* 122: 419–433.

Sokirko, A. V., V. Pastushenko, S. Svetina, and B. Zekš. 1994. Deformation of a lipid vesicle in an electric field: a theoretical study. *Bioelect. Bioenerg.* 34:101–107.

Song, J. and R. E. Waugh. 1993. Bending rigidity of SOPC membranes containing cholesterol. *Biophys. J.* 64:1967–1970.

Spector, A. A., W. E. Brownell, and A. S. Popel. 1998. Estimation of elastic moduli and bending stiffness of anisotropic outer hair cell wall. *J. Acoust. Soc. Am.* 103:1007–1011.

Spector, A. A., W. E. Brownell, and A. S. Popel. 1999a. Mechanical and electromotile characteristics of auditory outer hair cells. *Med. Biol. Eng. Comput.* 37:247–251.

Spector, A. A., W. E. Brownell, and A. S. Popel. 1999b. Nonlinear active force generation by cochlear outer hair cell. *J. Acoust. Soc. Am.* 105: 2414–2420.

Spector, A. A. 1999. Nonlinear electroelastic model for the composite outer hair cell wall. *ORL. J. Otorhinolaryngol. Relat. Spec. J.* 61: 287–293.

Strey, H., M. Peterson, and E. Sackmann. 1995. Measurement of erythrocyte membrane elasticity by flicker eigenmode decomposition. *Biophys. J.* 69:478–488.

Sun, K. 1997. Toward molecular mechanoelectric sensors: Flexoelectric sensitivity of lipid bilayers to structure, location, and orientation of bound amphiphilic ions. *J. Phys. Chem.* 101:6327–6330.

Sund, S. E., J. A. Swanson, and D. Axelrod. 1999. Cell membrane orientation visualized by polarized total internal reflection fluorescence. *Biophys. J.* 77:2266–2283.

Takashima, S. 1999. Computation of the dipole moment of protein molecules using protein databases. Bacteriophage T4 lysozyme and its mutants. *Colloids and Surfaces A: Physiochemical and Engineering Aspects.* 148:95–106.

Timoshenko, S. and S. Woinowsky-Kreiger. 1959. Theory of Plates and Shells. 2nd ed. McGraw Hill Book Co., New York.

Todorov, A. T., A. G. Petrov, and J. H. Fendler. 1994a. Flexoelectricity of charged and dipolar bilayer lipid membranes studied by stroboscopic interferometry. *Langmuir.* 10:2344–2350.

Todorov, A. T., A. G. Petrov, and J. H. Fendler. 1994b. First observation of the converse flexoelectric effect in bilayer lipid membranes. *J. Phys. Chem.* 98:3076–3079.

Tolomeo, J. A. and C. R. Steele. 1995. Orthotropic piezoelectric properties of the cochlear outer hair cell wall. *J. Acoust. Soc. Am.* 97:3006–3010.

Tolomeo, J. A., C. R. Steele, and M. C. Holley. 1996. Mechanical properties of the lateral cortex of mammalian auditory outer hair cells. *Biophys. J.* 71:421–429.

Ulfendahl, M. and N. Slepecky. 1988. Ultrastructural correlates of inner ear sensory cell shortening. *J. Submicrosc. Cytol. Pathol.* 20:47–51.

Waugh, R. E., J. Song, S. Svetina, and B. Zekš. 1992. Monolayer couplingand curvature elasticity in bilayer membranes by tether formation from lecithin vesicles. *Biophys. J.* 61:974–982.

Waugh, R. E. 1996. Elastic energy of curvature-driven bump formation on red blood cell membrane. *Biophys. J.* 70:1027–1035.

Xue, S., D. C. Mountain, and A. E. Hubbard. 1993. Direct measurements of electrically-evoked basilar membrane motion. *In:* Biophysics of Hair Cell Sensory Systems, H. Duifuis, J. W. Horst, P. van Dijk, and S. M. van Netten, eds. World Scientific, Singapore. 361–369.